Chemical Geology xxx (xxxx) xxx–xxx

Contents lists available at ScienceDirect

Chemical Geology

journal homepage: www.elsevier.com/locate/chemgeo

Cycles of trace elements and isotopes in the ocean – GEOTRACES and beyond

Limited impact of eolian and riverine sources on the biogeochemical cycling of Cd in the tropical Atlantic☆

Ruifang C. Xie[a,*,1], Stephen J.G. Galer[a], Wafa Abouchami[b,2], Martin Frank[c]

[a] Max Planck Institute for Chemistry, Climate Geochemistry Department, Hahn-Meitner-Weg 1, 55128 Mainz, Germany
[b] Institut de Physique du Globe de Paris, 1 rue Jussieu, 75238 Paris cedex 05, France
[c] GEOMAR Helmholtz Center for Ocean Research Kiel, Wischhofstrasse 1-3, 24148 Kiel, Germany

ARTICLE INFO

Editor: Michael E. B

Keywords:
GEOTRACES
Tropical Atlantic Ocean
Cadmium isotopes
Saharan dust
Oxygen-deficient waters
Amazon River

ABSTRACT

We present coupled cadmium (Cd) concentrations and Cd isotopic compositions (expressed as δ^{114}Cd) in seawater profiles along the northeast-southwest GEOTRACES GA11 section in the tropical Atlantic Ocean. The GA11 section encompasses three contrasting regions including the Amazon River plume, the North African dust plume, and the Guinea Dome oxygen deficient zone (ODZ). Given the long oceanic residence time of Cd (10^4 to 10^5 yr), local inputs such as atmospheric and riverine sources are generally considered to be of little importance for the open ocean Cd budget, and the limited Cd isotope dataset available thus far has prevented any unambiguous conclusions on the importance of these processes. The GA11 section is ideally located for assessing the influence of external, natural and anthropogenic riverine and eolian inputs, as well as internal processes, on the Cd mass balance in the tropical Atlantic Ocean. As in previous Cd isotope studies, this dataset documents that both surface consumption–regeneration of micronutrients within the water column and deep water mass mixing exert the prime control on the cycling of Cd. However, we do observe some near-surface samples with lower-than-expected δ^{114}Cd signatures along the western section of the transect. Surface waters sampled at the margin of the Amazon freshwater plume show no resolvable difference in [Cd] and δ^{114}Cd compared to waters outside of the plume, suggesting that the Amazon River is not an important source of Cd to the open ocean. Although the eastern GA11 transect is directly downwind of the Saharan dust plume, atmospheric Cd deposition accounts for < 1% of the inferred upwelling flux, indicating that atmospheric inputs to the surface North Atlantic Ocean, even within the main Saharan dust plume, only have a relatively minor influence on the Cd budget. In the subsurface tropical Atlantic (100–200 m water depth), there is a clear deviation from a tight linear Cd-PO_4 correlation toward lower Cd concentrations for a given PO_4 concentration. Our new Cd data show that this Cd-PO_4 decoupling is likely a feature of the entire tropical Atlantic and may possibly reflect PO_4 enrichment via preferential re-mineralization of organically-bound phosphorus. Alternatively, the decoupling may arise from subsurface Cd depletion caused by precipitation of Cd sulphide within sinking organic particulate microenvironments, as has been suggested in recent studies.

1. Introduction

Recent marine cadmium (Cd) isotope studies have offered new insights into the mechanisms governing the marine cycling of the micronutrient Cd and its isotopes. Phytoplankton utilization of Cd in the Southern Ocean closely follows a closed-system Rayleigh fractionation model (Abouchami et al., 2011; Abouchami et al., 2014; Xue et al., 2013). In Cd-deficient ([Cd] < 0.1 nmol kg^{-1}) surface waters in other oceanic regions, however, Cd isotopic compositions (hereafter expressed as δ^{114}Cd) are relatively uniform (Janssen et al., 2017; Gault-Ringold et al., 2012; Sieber et al., 2018; Xie et al., 2017), except for a few surface samples in the North Pacific and North Atlantic where highly fractionated δ^{114}Cd values have been reported (Conway and John, 2015a; Conway and John, 2015b; Ripperger et al., 2007; Xue

☆ This article is part of a special issue: "Cycles of trace elements and isotopes in the ocean – GEOTRACES and beyond" - edited by Tim M. Conway, Tristan Horner, Yves Plancherel, and Aridane G. González.

* Corresponding author.
E-mail addresses: rxie@geomar.de (R.C. Xie), steve.galer@mpic.de (S.J.G. Galer), wabouchami@ipgp.fr (W. Abouchami), mfrank@geomar.de (M. Frank).
[1] Present address: GEOMAR Helmholtz Center for Ocean Research Kiel, Wischhofstrasse 1-3, 24148 Kiel, Germany.
[2] Present address: Institut für Geologie und Mineralogie, Universität zu Köln, Zülpicher Str. 49b, 50674 Köln, Germany.

https://doi.org/10.1016/j.chemgeo.2018.10.018
Received 4 April 2018; Received in revised form 14 October 2018; Accepted 19 October 2018

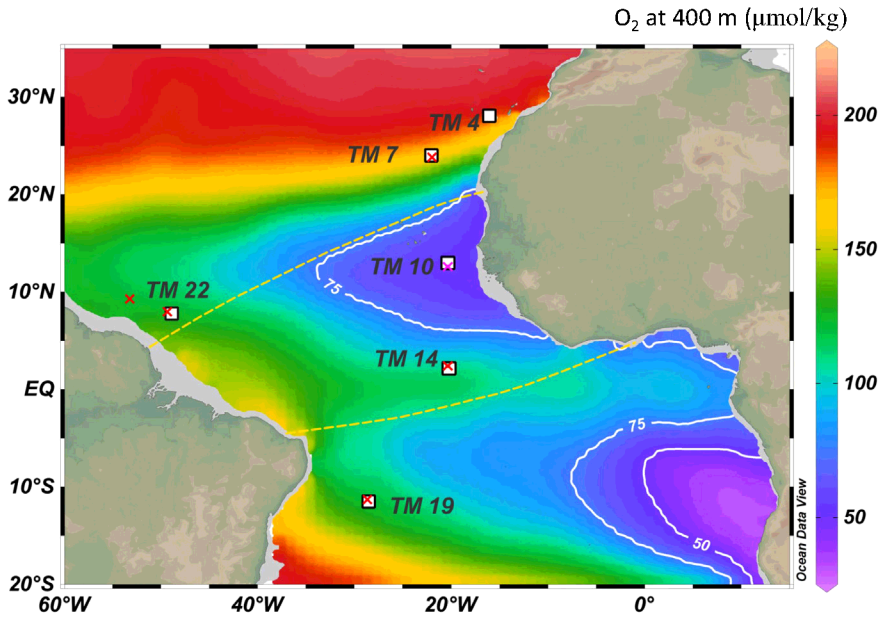

Fig. 1. Locations of Cd water profiles (open squares) and towed-Fish surface sites (red crosses) in the tropical Atlantic along the GEOTRACES GA11 section. Colored contours reflect oxygen concentrations at 400 m depth, with the 75 µmol kg^{-1} contour line highlighting areas of oxygen-deficient waters (Garcia et al., 2014). Yellow dashed lines show schematically the main transport pathway of African dust across the Atlantic. This map was produced using Ocean Data View (Schlitzer, 2014). (For interpretation of the references to color in this figure legend, the reader is referred to the web version of this article.)

et al., 2012). This uniformity can be explained by biological uptake of Cd in a simple open system, steady-state model for the surface mixed layer (Janssen et al., 2017; Xie et al., 2017). Alternatively, Xie et al. (2017) hypothesized that organically-complexed Cd in these Cd-deficient regions might dominate the dissolved pool (filtered < 0.2 µm) and buffer surface water δ^{114}Cd to low values upon utilization of the dissolved Cd pool. In the intermediate and deep ocean, by contrast, seawater δ^{114}Cd has been shown to follow the large-scale ocean circulation and water mass mixing making it potentially a promising proxy for reconstructing past deep water circulation (Abouchami et al., 2014; Sieber et al., 2018; Xie et al., 2017; Yang et al., 2018).

In hypoxic waters in the upper oxygen-deficient zones (ODZ) and in the overlying oxycline waters, it has been proposed that isotopically light Cd is removed as precipitates of cadmium sulphide (CdS), resulting in depleted dissolved Cd relative to PO_4 (Conway and John, 2015a; Janssen et al., 2017; Janssen et al., 2014; Waeles et al., 2013). As a result, particles collected in oxygen-deficient waters are then expected to display lighter δ^{114}Cd (Janssen et al., 2014), which has been confirmed in precipitation experiments by Guinoiseau et al. (2018). Supporting recent inferences (Janssen et al., 2014; Conway and John, 2015a), Bianchi et al. (2018) have modelled that CdS precipitation most likely occurs at the top of the ODZ, and additionally depends strongly on the particle size distribution of sinking organic matter.

Cadmium has a long, but uncertain, oceanic residence time – estimated at 2×10^4 (Martin and Whitfield, 1983) to 3×10^5 years (Li, 1982) – and is largely supplied to the surface ocean from underlying waters (Bruland, 1980). Consequently, local atmospheric and riverine inputs of natural Cd are not expected to impact significantly the global ocean Cd budget (Bruland, 1980; Boyle et al., 1982; Duce et al., 1991). But, our current understanding of the ocean cycling of Cd is limited by the paucity of Cd isotope data for anthropogenic and natural input sources. Emissions of Cd originating from non-ferrous metal production and fossil fuel burning (Cullen and Maldonado, 2013; and references therein) are the dominant sources of anthropogenic Cd to the atmosphere and rivers, and ultimately the ocean. To date, there are only two studies that have reported Cd isotopic compositions of eolian materials. First, loess samples have an average δ^{114}Cd of −0.02 ± 0.08‰ (2SD, n = 3) (Schmitt et al., 2009); second, recent data on bulk African dust collected on research vessels in the tropical Atlantic span a larger range in values from −0.19 ± 0.15‰ to +0.14 ± 0.13‰, indistinguishable from that of the anthropogenic (leachable) dust fraction (Bridgestock et al., 2017). By comparison, industrial dust derived from Pb-Zn refineries, with δ^{114}Cd ranging from −0.10 to −0.74‰, is isotopically "light", which is considered to be a unique signature of anthropogenic sources (Chrastný et al., 2015; Cloquet et al., 2006).

Major rivers exhibit a rather large spread in dissolved Cd concentrations, ranging between 0.005 and 3.7 nmol L^{-1} (Gaillardet et al., 2014; Viers et al., 2009; and references therein), but few Cd isotope data on rivers have been published thus far. A study on brackish waters (salinity < 10) on the Siberian Shelf yielded Cd isotopic compositions of δ^{114}Cd = 0.32 ± 0.12‰ (2SD, n = 7) (Lambelet et al., 2013), heavier than those of the Bulk Silicate Earth (δ^{114}Cd = −0.04 ± 0.02‰, 2SD, n = 7) (Schmitt et al., 2009). River sediments downstream of Pb-Zn refineries are generally enriched in heavy Cd isotopes (δ^{114}Cd = +0.26 ± 0.12‰, 2SD, n = 7; Cloquet et al., 2006; Gao et al., 2008; Gao et al., 2013), though industrially polluted soil in the vicinity of these refineries have Cd isotopic compositions that are quite variable (δ^{114}Cd = −0.76‰ to +0.10‰) (Cloquet et al., 2006). It has recently been suggested that natural weathering results in a large Cd isotope fractionation between stream sediments and river bank soil, with an isotopic difference $\Delta^{114}Cd_{(stream\ sediment\ -\ soil)}$ of up to 0.5‰ (Zhang et al., 2016). In addition, large isotopic differences between river water and underlying sediments ($\Delta^{114}Cd_{(river\ -\ sediment)} \sim 0.9–1.6‰$) have also been observed (Yang et al., 2019). Thus, the riverine dissolved Cd isotopic compositions might strongly depend on the local geologic settings and anthropogenic input, and remains to be adequately characterized.

The main objectives of this study are to evaluate (1) the relative importance of Cd inputs via atmospheric and riverine pathways for the oceanic Cd mass balance, building on earlier studies (e.g. Bruland, 1980; Boyle et al., 1982; Duce et al., 1991) and (2) potential sinks for Cd in oxygen depleted waters. We measured dissolved Cd concentrations ([Cd]) and δ^{114}Cd along with macronutrients in sixty-three seawater samples collected on board the German RV Meteor in spring 2010, along the GEOTRACES GA11 section from Las Palmas (Canary Islands, Spain) to Trinidad and Tobago (Fig. 1). The GA11 section includes three regions that are ideal for assessing the significance of external Cd sources (rivers and dust) and sinks (ODZ) in the tropical North Atlantic. These regions are (1) the surface western tropical Atlantic downstream of the world's largest river - the Amazon River (riverine input); (2) the surface eastern tropical Atlantic Ocean directly below the African dust plume (atmospheric input); and (3) the subsurface ODZ of the eastern tropical North Atlantic (a potential Cd sink).

2. Material and methods

2.1. Seawater sampling

Seawater for Cd isotope analysis was sampled at six stations using Go-Flo water samplers mounted on a trace-metal-clean rosette. Six surface samples were collected underway along the transect using a trace-metal-clean Fish sampler towed at a depth of 2–3 m. After sample collection, seawater was filtered on board through 0.22 µm filter capsules (Sartobran, Sartorius) into high-density polyethylene bottles and canisters that had previously been cleaned with hot 6 N HCl. Seawater samples were acidified to pH ~2 with ultra-clean 12 M HCl (Baseline, Seastar) immediately after filtration. Both filtration and acidification were performed in a clean room laboratory container on board the ship.

2.2. Nutrient measurements

Inorganic nutrients (nitrate, phosphate and silica) were determined on small aliquots of the filtered, acidified seawater samples at the Royal Netherlands Institute for Sea Research (NIOZ, Texel) using a Bran and Luebbe Traacs-800+ Auto-analyzer, following slightly modified procedures of Grasshoff et al. (2009). Further details about the methodology can be found in Middag et al. (2009).

2.3. Cd isotope analysis

Chemical separation of Cd from the seawater samples was carried out at the Max Planck Institute for Chemistry in Mainz. A mixed ^{106}Cd-^{108}Cd double spike was added beforehand in order to correct for instrumental mass bias and any fractionation induced during chemical processing (Schmitt et al., 2009). Detailed chemistry protocols for small ($\leq$1 L) and large (2 − 10 L) quantity seawater samples follow those previously described (Abouchami et al., 2011; Xie et al., 2017). The total procedural blank during a two-year period (including the period of this study) was below 9 pg for the 1 L column chemistry and indistinguishable from the MQ blank for the 2-10 L column chemistry.

Cadmium isotopic compositions were measured on a ThermoFisher Triton Thermal Ionization Mass Spectrometer (TIMS) running in static multi-collection mode. Cadmium concentration data were obtained by isotope dilution, using the mass bias-corrected ^{106}Cd/^{112}Cd ratios. The reference material NIST SRM-3108 was analyzed alongside each batch of samples, with the amount of Cd loaded adjusted to match that of the samples analyzed. The reproducibility of NIST SRM-3108 ranged from 50 ppm for a load size of 1 ng to 10 ppm for a load size of 100 ng (see Xie et al., 2017). The average Cd isotopic composition of NIST SRM-3108 is consistent with the consensus value (Abouchami et al., 2013), and duplicate analyses of the SAFe standard reported in Xie et al. (2017) agree within error with accepted GEOTRACES consensus values (www.geotraces.org).

Cadmium isotopic compositions were obtained by measuring the ^{112}Cd/^{110}Cd ratio and are reported in Supplementary Tables S1 and S2 in both $\varepsilon^{112/110}$Cd and δ^{114}Cd notations (using the inter-conversion factor reported by Abouchami et al., 2013) relative to the NIST SRM-3108 standard. Both Cd concentrations and isotopic compositions are also available through the GEOTRACES IDP2017 (Schlitzer et al., 2018). The δ^{114}Cd represents the deviation in parts per thousand in ^{114}Cd/^{110}Cd of the sample relative to that of NIST SRM-3108, i.e.

$$\delta^{114}\mathrm{Cd}\ (‰) = \left(\frac{(^{114}\mathrm{Cd}/^{110}\mathrm{Cd})_{\mathrm{sample}}}{(^{114}\mathrm{Cd}/^{110}\mathrm{Cd})_{\mathrm{NIST}}} - 1\right) \times 1000 \quad (1)$$

3. Results

3.1. Distribution of macronutrients

Data for macronutrients PO_4, NO_3 and Si are reported in Supplementary Tables S1 and S2. The distributions of PO_4 and NO_3 show a typical uptake-re-mineralization pattern and are tightly coupled with each other (Fig. S1). Silica concentrations, on the other hand, display two distinct correlations with PO_4 and NO_3: a steeper linear correlation of PO_4:Si or NO_3:Si for samples shallower than 1500 m and a shallower linear correlation for deeper samples (Fig. S2). The deeper samples have higher [Si] for a given [PO_4] or [NO_3], indicative of the influence of Si-rich Southern Ocean deep waters flowing northwards into the tropical Atlantic Ocean.

3.2. Vertical distribution of [Cd] and Cd isotopes

3.2.1. Comparison at cross-over stations GA11-GA03-GA02

The GA11 cruise shared two cross-over stations – one with the U.S. GEOTRACES cruise GA03 in the eastern Atlantic (station USGT10-07; Conway and John, 2015a) and the other with the Dutch GEOTRACES cruise GA02 in the western Atlantic (station GA02-36; Middag et al., 2018). Measured Cd concentrations at the GA11 and GA02 crossover stations show excellent agreement (Fig. S3a), regardless of differences in Cd separation chemistry and in techniques used in the two laboratories. Cadmium concentrations and isotopic compositions for the GA03 and GA11 crossover stations generally agree well (Fig. S3b) but for the surface waters, small differences (outside of analytical uncertainty) in δ^{114}Cd likely reflect inter-annual biogeochemical variability in the surface and subsurface waters. Alternatively, analytical artifacts due to the low amounts of Cd available in the surface water samples, as well as differences in measurement methodologies, might also contribute to the observed discrepancy (Janssen et al., 2017; Xie et al., 2017). Inter-laboratory comparison of common low-level Cd seawater samples is needed to resolve this issue.

3.2.2. Depth profiles at GA11

Fig. 2 reports the depth profiles of [Cd] and δ^{114}Cd along the GA11 section. These exhibit generally antithetic distributions, with depleted [Cd] and heavy δ^{114}Cd at the surface, while increasing [Cd] and decreasing δ^{114}Cd occur with depth. These distributions primarily reflect biological utilization in the surface ocean, during which preferential uptake of the lighter Cd isotopes and subsequent organic matter export and re-mineralization at depth occur, consistent with previous Cd isotope studies (e.g. Abouchami et al., 2011; Ripperger et al., 2007).

Along the GA11 section, Cd-depleted surface waters (all tow-fish samples, except TM4) have a [Cd] range of ~0.8 to 4.5 pmol kg^{-1} while those from the eastern basin have isotopically heavier Cd (δ^{114}Cd = +0.26‰ to +0.38‰, n = 3) than those from the western basin (δ^{114}Cd = −0.60‰ to +0.14‰, n = 3) (Tables S1 and S2; Fig. 3). These values are overall at the lower end of the range reported so far for global surface waters (see summary in Xie et al., 2017).

Subsurface waters (10–100 m), however, exhibit markedly heavier δ^{114}Cd between +0.54‰ and +0.70‰ (Fig. 2), within the range of existing literature data compiled by Xie et al. (2017). Toward the surface, shifts of ~0.2‰ to lower values are observed at stations TM4, TM7 and TM10 along the eastern GA11 section (Fig. 2, Tables S1 and S2). At stations TM 19 and TM22, surface signatures even show negative values (Fig. 2, Tables S1 and S2).

At intermediate depths and the deep ocean (> 1000 m), [Cd] and δ^{114}Cd systematically track the water mass distribution (Fig. 4). Low [Cd] (~0.28 to 0.37 nmol kg^{-1}) and isotopically heavy Cd (δ^{114}Cd ≈ +0.32‰ to +0.48‰) are associated with northern-sourced waters (Boyle et al., 2012; Conway and John, 2015a). In contrast, high [Cd] (~0.50 to 0.69 nmol kg^{-1}) and lighter Cd (δ^{114}Cd ≈ +0.28‰) reflect the presence of AABW, while high [Cd] (~0.53 to

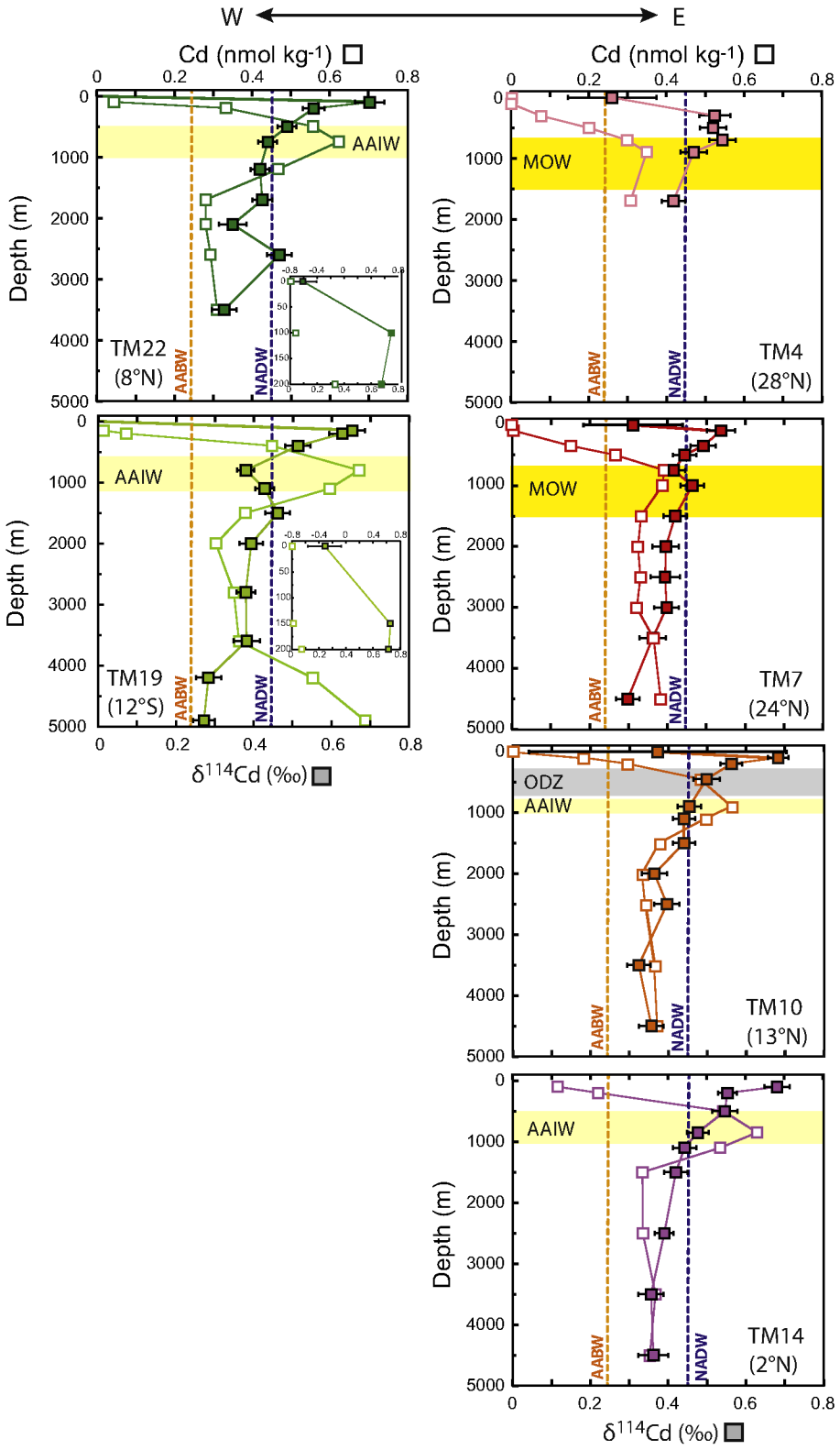

Fig. 2. Profiles of Cd concentration (top axis; open symbols) and δ^{114}Cd (bottom axis; solid symbols) for stations TM4 (pink), TM7 (red), TM10 (orange), TM14 (purple), TM19 (light green), and TM22 (dark green) along the GA11 section. Surface δ^{114}Cd data plotted for TM7, TM10, TM19 (inset) and TM22 (inset) are from nearby towed-Fish sites along this transect. Water mass acronyms are: AAIW – Antarctic Intermediate Water, MOW – Mediterranean Overflow Water, NADW – North Atlantic Deep Water, AABW – Antarctic Bottom Water. Dashed lines indicate endmember δ^{114}Cd values for AABW (orange) and NADW (blue). The depth ranges are marked for intermediate waters AAIW (light yellow) and MOW (bright yellow). The oxygen-deficient zone at station TM10 is highlighted by grey shading. (For interpretation of the references to color in this figure legend, the reader is referred to the web version of this article.)

0.60 nmol kg^{-1}) and heavier Cd (δ^{114}Cd ≈ +0.44‰) are characteristic features of AAIW (Abouchami et al., 2014; Xie et al., 2017).

4. Discussion

4.1. Deep and intermediate water mass mixing

The deep and intermediate water dataset presented here is consistent with simple binary mixing between NADW and southern-sourced waters (Fig. 4). Although bottom waters from stations TM22

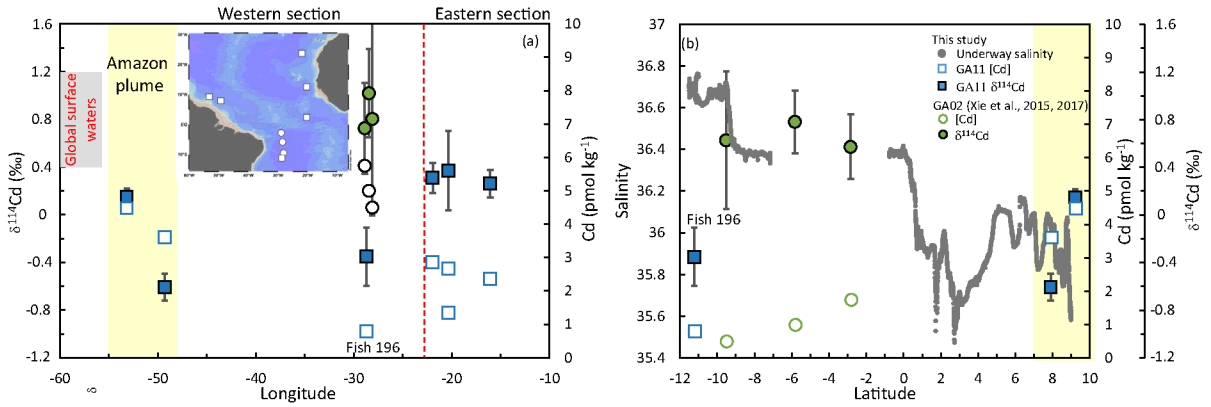

Fig. 3. (a) Surface Cd concentrations (open symbols) and δ^{114}Cd (solid symbols) in the tropical Atlantic from 60°W to 10°W. Circles are data from Xie et al. (2015, 2017), and squares are data reported in this study. A red dashed line separates samples along the western section to the left from those along the eastern section to the right. Yellow shading indicates where the Amazon plume was seen. Grey box highlights the global average δ^{114}Cd values in Cd-deficient surface waters (Xie et al., 2017). Inset map shows location of the Fish samples. (b) Surface Cd concentrations (open symbols), δ^{114}Cd (solid symbols) and GA11 underway salinity (grey lines) along the western tropical Atlantic from 12°S to 10°N. (For interpretation of the references to color in this figure legend, the reader is referred to the web version of this article.)

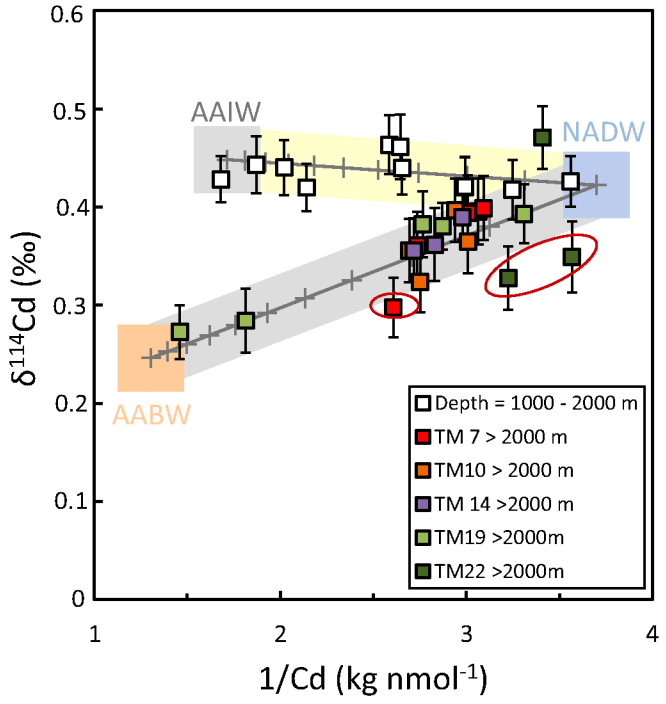

Fig. 4. Cross plot of δ^{114}Cd versus the reciprocal of [Cd] demonstrating that both parameters are consistent with binary water mass mixing between AAIW/AABW and NADW. Samples are subdivided into those deeper than 2000 m (solid colored squares) and those at 1000–2000 m (open squares). Colored boxes indicate water mass endmember values. We include an error (2SE) of δ^{114}Cd = 0.03‰, typically seen for deep seawater samples, for the water mass endmembers as shown in grey (AABA-NADW mixing) and yellow shadings (AAIW-NADW mixing). (For interpretation of the references to color in this figure legend, the reader is referred to the web version of this article.)

(2100–3500 m) and TM7 (4500 m) do not strictly lie on the NADW-AABW mixing line, they are still within error allowing for some variability in the endmember compositions. At the northernmost stations TM7 and TM10 in the eastern basin, which overlap with the US GA03 section, our Cd isotope data show that deep waters contain 10 to 20% of AABW, in agreement with the water mass distribution and estimates deduced from a multi-parameter water mass characterization of this region (Jenkins et al., 2015).

The control of water mass mixing on the distribution of Cd and its isotopes in the intermediate and deep ocean was first demonstrated by Abouchami et al. (2014) in the eastern South Atlantic and also observed along the western boundary in the South Atlantic (Xie et al., 2017), the North Atlantic (Conway and John, 2015a; Roshan and Wu, 2015; Yang et al., 2018), as well as the South Pacific (Sieber et al., 2018). Our present study lends additional support to the potential utility of δ^{114}Cd as a water mass tracer in the intermediate and deep ocean.

4.2. Influence of Amazon riverine Cd inputs to surface waters

The northern part of the western GA11 section encountered the edge of the Amazon River low-salinity surface water plume. The mean dissolved [Cd] in the Amazon River is ~0.18 μg L^{-1} (~1.6 nmol L^{-1}) (Seyler and Boaventura, 2003; Gaillardet et al., 2014), which is about 2 to 3-fold higher than that of global average deep waters (e.g. Abouchami et al., 2014). But this value may not necessarily be representative of the Cd input reaching the open ocean after estuarine mixing. The Cd concentration within the Amazon plume itself varies between 0.05 and 0.1 nmol kg^{-1} (Boyle et al., 1982), and is therefore similar to that measured in global surface and subsurface waters.

Our surface waters sampled at the margin of the Amazon plume display no pronounced increase in [Cd] (3.6–4.5 pmol kg^{-1}; Fig. 3a) compared to surface concentrations found in the western South Atlantic (1.0–2.0 pmol kg^{-1}) sampled during the GA02 cruise (Middag et al., 2018; Xie et al., 2015). This is consistent with the surface salinity of our samples at the margin of the Amazon plume along our transect, only being slightly fresher (S as low as 35.6) than waters outside the plume (S ≈ 36.1). This implies Amazon river water contribution of < 2% to ambient seawater at our stations. Based on the combination of the relatively low [Cd] within the main Amazon plume (Boyle et al., 1982) and the small fraction of Amazon river water sampled at our Station TM22 at the margin of the plume, we suggest that Cd input from the Amazon did not measurably affect this site. This is consistent with the general conclusions of Boyle et al. (1982) that riverine Cd does not reach the open ocean in significant amounts. Likewise, the co-variation of Cd and salinity in surface waters collected in and out of the influence of the Amazon plume (22 < S < 36) observed by Tovar-Sanchez and Sañudo-Wilhelmy (2011) suggests that Amazon River inputs merely act to dilute ambient open ocean Cd concentrations.

Additional Cd isotope studies covering the entire salinity range between river water and open ocean surface waters and including particulate material, are needed to quantify reliably potential riverine Cd contributions, if any. Similarly, the large seasonal variability in the

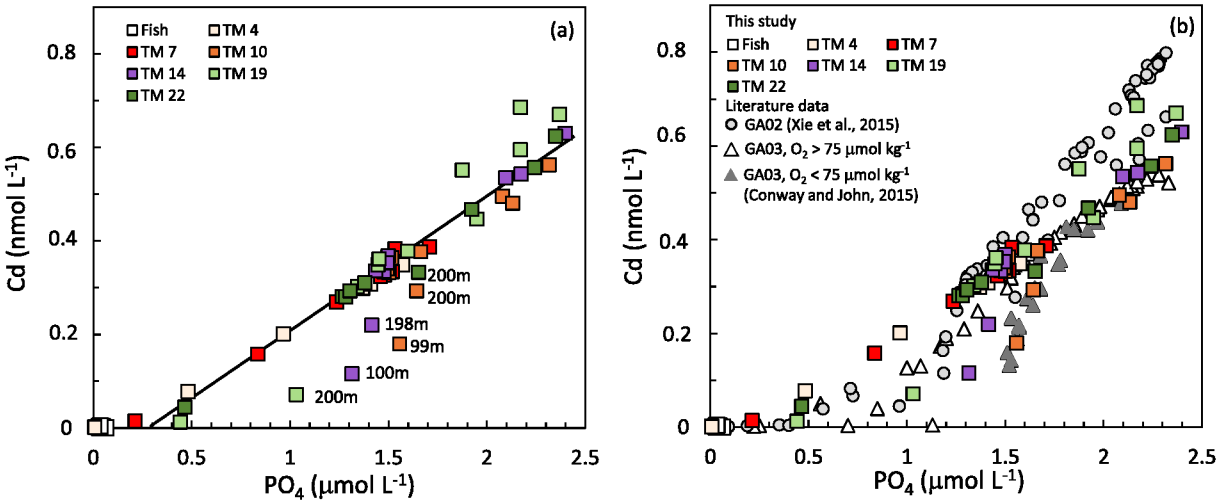

Fig. 5. Cross plots of dissolved Cd vs. PO_4 are shown (a) for GA11 stations only and (b) for GA11 (this study), GA02 (grey circles; Xie et al., 2015) and GA03 ODZ stations (open and dark grey triangles; Conway and John, 2015a, 2015b). The solid black line in (a) highlights schematically the tight linear correlation between Cd and PO_4.

riverine Cd concentration in the Amazon Basin correlates strongly with discharge (Seyler and Boaventura, 2003), further complicating assessment of the Amazon River Cd contribution to the open ocean. For example, the extent of estuarine sequestration of Cd remains very uncertain (Boyle et al., 1982).

We note that the δ^{114}Cd signatures of the two plume samples and that of FISH 196 located outside of the plume (Fig. 3a), are much lower (−0.61‰ to +0.15‰) than those of nearby tow-fish samples in the western South Atlantic (+0.4‰ to +1‰; Xie et al., 2017). Although unlikely, such low δ^{114}Cd values might conceivably originate from contamination of the low [Cd] surface waters during sampling, which cannot be entirely ruled out. The origins of these light surface δ^{114}Cd values in the tropical western Atlantic thus remain ambiguous but the small riverine fractions in our surface samples and the fact that also data outside the plume have very low δ^{114}Cd values clearly show that the Amazon River is unlikely to be the source of the light Cd to the western Atlantic surface ocean.

4.3. Can Saharan dust explain the light Cd isotope signature in the surface eastern tropical Atlantic?

The decrease in δ^{114}Cd from subsurface to surface at stations TM4, TM7 and TM10 (Fig. 2) might be attributable to eolian inputs of African dust given the location of these stations downwind of the Saharan dust plume. These lower surface δ^{114}Cd values of +0.26‰ to +0.38‰ are not, however, at odds with the global compilation of dissolved Cd isotope signatures in Cd-deficient waters ([Cd] < 0.1 nmol kg^{-1}) (Xie et al., 2017). In fact, the slight decrease in δ^{114}Cd from subsurface to surface waters – which generally correlates with the depths of the Chl-a maxima – has been observed previously in the western South Atlantic (Xie et al., 2017), the tropical North Atlantic (Conway and John, 2015a), and the South Pacific (Sieber et al., 2018), albeit the surface and subsurface δ^{114}Cd values were often within error of one another.

Mineral dust supply to the eastern tropical North Atlantic Ocean has been shown to be an important source of micronutrients promoting nitrogen fixation (Mills et al., 2004). However, recent studies have argued that atmospheric inputs do not significantly impact the surface ocean Cd budget (Bridgestock et al., 2017; Waeles et al., 2016). To investigate the role of atmospheric Cd in the GA11 section, we used the same approach as used in Xie et al. (2017). Briefly, the atmospheric Fe deposition flux in the eastern tropical North Atlantic is 0.2–2 ng m^{-2} yr^{-1} (also expressed as an atmospheric loading of 1–10 µg m^{-3}) as reviewed and summarized in Mahowald et al. (2009). Using a mean upper continental crustal Cd/Fe of 2.88 µg g^{-1} (Taylor and McLennan, 1985), the atmospheric Cd deposition flux in this region is estimated to be 0.6–6 µg m^{-2} yr^{-1} (or a load of 3–30 pg m^{-3}). The estimated atmospheric Cd load agrees well with that measured (4–40 pg m^{-3}) along the GEOTRACES GA06 section by Bridgestock et al. (2017) proximal to our study sites.

We compare this eolian Cd flux with that expected from upwelling in the water column (see Xie et al., 2017), assuming that nearly all (> 80%) of this mineral-hosted Cd is soluble (Duce et al., 1991). The upwelling velocity in the tropical North Atlantic has been estimated at 10–17 m yr^{-1}, based on a ^{14}C-derived vertical volume transport of 4–7 Sv (Wunsch, 1984) and a surface ocean area of ~1.3 × 10^{13} m^2 in the box delimited by [0°, 60°W, 16°N, 10°E]. Using a mean [Cd] of 0.5 nmol kg^{-1} at the base of the thermocline and assuming a seawater density of 1000 kg m^{-3}, the upwelled Cd flux in the tropical North Atlantic is estimated to be 550–950 µg m^{-2} yr^{-1}. Thus, the upwelling Cd flux is at least 90-fold greater than the eolian Cd deposition flux based on spot measurements (Bridgestock et al., 2017) and long-term estimates (this study). Altogether, atmospheric deposition of Cd, even under the Saharan dust plume, appears to be of less importance than upwelling in supplying Cd to surface waters in the tropical Atlantic.

4.4. Cd-PO_4 decoupling in the tropical Atlantic

The eastern tropical North Atlantic features an intense, wind-driven upwelling region known as the Guinea Dome where enhanced primary productivity takes place. A pronounced body of oxygen-deficient waters prevails in the subsurface as a result of enhanced re-mineralization of organic matter. In this region, oxygen concentrations in the upper thermocline (300–700 m) often drop below 100 µmol kg^{-1} but generally remain above ~40 µmol kg^{-1} (Karstensen et al., 2008). Compared to the ODZs of the eastern Pacific and the Indian Oceans – where oxygen concentrations reach as low as a few µmol kg^{-1} – the Guinea Dome oxygen-deficient waters are significantly more oxygenated. As in previous studies from the same general area (see Conway and John, 2015a; Janssen et al., 2014), we will consider waters with $[O_2]$ < 75 µmol kg^{-1} as being "oxygen deficient".

A cross-plot of Cd vs. PO_4 shows that the majority of the GA11 data exhibit a tight linear Cd-PO_4 correlation (schematic black line in Fig. 5a). For samples with PO_4 > 1.2 µmol kg^{-1}, our data are consistent with those from ODZ stations along the GA03 North Atlantic zonal transect (Conway and John, 2015a) (Fig. 5b). A few deviations from the main linear trend can be seen in Fig. 5b for some samples.

These include: (1) the very surface samples where Cd concentrations exhibit extreme depletion; (2) waters at 100–200 m at stations TM10, TM14 and TM19, which show a Cd depletion relative to PO_4; and (3) intermediate (800–1100 m) and deep (> 4000 m) waters from station 19 where Cd is enriched relative to PO_4.

The intermediate and deep waters with higher [Cd] at station 19 (11.5°S) in the western tropical Atlantic appear to be "pulled" toward the GA02 western South Atlantic dataset (Xie et al., 2015) (Fig. 5b), and can be interpreted as reflecting the influence of Cd-rich AAIW and AABW. This influence is not as pronounced at station TM22 at 7.8°N, presumably due to its more northerly location.

In the following, we discuss plausible mechanisms that could account for the observed decoupling between Cd and PO_4, and stress that combined particulate and dissolved data from future studies will be key for distinguishing between these mechanisms in different oceanic regions.

4.4.1. The CdS hypothesis within ODZ waters

The lower-than-expected [Cd] for a given PO_4 at stations TM10, TM14 and TM19 in this study overlaps with the data of the GA03 samples with $[O_2] < 75\,\mu mol\,kg^{-1}$ (see Conway and John, 2015a; Janssen et al., 2014) (Fig. 5b). The significant Cd depletion of 20 to 80% relative to PO_4 reported previously within the Guinea Dome ODZ was attributed to the precipitation of authigenic CdS within organic matter micro-environments (Conway and John, 2015a; Janssen et al., 2014). Sulphides tend to preferentially incorporate isotopically light Cd, as demonstrated by analyses of oceanic hydrothermal sulphides (Schmitt et al., 2009), as well as ab-initio calculations (Yang et al., 2015) and recent seawater CdS precipitation experiments (Guinoiseau et al., 2018).

Our new dataset from the GA11 transect suggests that if CdS precipitation is an important Cd sink in oxygen deficient waters, then this process must occur in the shallow water depth range of 100–200 m within the upper ODZ (see Fig. 5). This would be in agreement with previous observations in other ODZs (Conway and John, 2015a; Janssen et al., 2014; Xie et al., in review) and modelling simulations (Bianchi et al., 2018).

The modelling study by Bianchi et al. (2018) has shown that large (millimeter-sized) organic particles within the Guinea Dome can maintain a sulphate-reducing core, providing sufficient in-situ H_2S to bind Cd as sulphide. These authors additionally modelled the profiles of particulate Cd/P, which agree well with those actually measured (Conway and John, 2015a; Janssen et al., 2014), providing strong support for authigenic precipitation of CdS within the upper parts of the ODZ. The fate of CdS hosted in particulates sinking within more oxygenated waters below the ODZ is controversial, however (see discussion in Guinoiseau et al., 2018).

4.4.2. Lower Cd/PO_4 remineralization ratios in the tropical Atlantic

Data from both the GA03 cruise in the eastern tropical North Atlantic (Conway and John, 2015a) and GA11 show that the largest Cd depletion occurs in the depth range of 100–200 m at the tropical stations only (Fig. 5b), suggesting that Cd depletion might be a common feature of the subsurface tropical Atlantic. This inference is consistent with studies from the GA02 section in the western Atlantic that also found an offset to lower subsurface Cd relative to PO_4 in the tropical and subtropical regions (Middag et al., 2018; Xie et al., 2015).

We propose that the feature of lower-than-expected Cd for a given PO_4 in the subsurface tropical Atlantic may alternatively reflect changes in Cd/P remineralization ratios. This hypothesis is in line with a recent study by Middag et al. (2018) who proposed a similar mechanism whereby Cd/P remineralization ratios are likely to be lower in highly oxygen deficient waters from the tropical Atlantic. In our dataset, regenerated PO_4, calculated from AOU (Apparent Oxygen Utilization), shows higher values at shallower depth at the tropical stations (TM10, TM14 and TM19) than at northern stations TM4 and TM7 (Fig. S4). This seems to indicate that PO_4 is respired faster in the subsurface of the tropical Atlantic. Particulate Cd data are unfortunately scarce in our study area. However, particulates collected using surface-tethered sediment traps in the Guinea Dome have ratios of particulate organic carbon (POC) to phosphorus (POP), as well as particulate organic nitrogen (PON) to POP ratios, that are significantly higher in the top 300 m than are found in deeper samples (Engel et al., 2017). This, in turn, would imply preferential re-mineralization of POP relative to POC and PON in the upper 300 m. Limited evidence from the central and high-latitude North Atlantic showed an increased affinity of Cd for POP (Cd:POP = 0.5 mmol/mol) compared to that for POC (Cd:POC = 3 μmol/mol) (Kuss and Kremling, 1999). However, labile particulate Cd/P ratios in the eastern tropical Atlantic tend to increase from the surface toward the subsurface (~150 m), and may reflect differential re-mineralization of Cd and P in sinking particulates (Twining et al., 2015). Furthermore, particulate P is shown to explain only 49% of the variability of particulate Cd in the surface North Atlantic, likely a result of differential remineralization of Cd and P or changes in metal/P stoichiometries in plankton (Twining et al., 2015).

The lower Cd/P remineralization ratios may be a result of depth-dependent re-mineralization of Cd-poor suspended organic matter at shallow depths and Cd-rich ballasted (by biogenic $CaCO_3$) sinking organic matter in the deeper ocean (Wu and Roshan, 2015). If sinking particulates do indeed have higher Cd/P ratios, this idea may possibly apply to the entire tropical Atlantic, where biogenic carbonate represents 40–80% of the total sinking particulates collected at ~600 m depth (Fischer and Karakaş, 2009).

In the intense Peruvian ODZ, Cd/P ratios of prokaryotes were found to be significantly higher than those of the mixed layer biomass (Ohnemus et al., 2017), causing a slight depletion of Cd in ambient seawater (John et al., 2017). If such a shift from autotrophic to heterotrophic biomass also occurs in the Guinea Dome ODZ, this would likely also affect the seawater distribution of Cd, its isotopes and PO_4 in seawater. Future studies on Cd/P ratios in suspended and sinking particulates in the global ocean will certainly provide important insights into this issue.

4.4.3. $Cd\text{-}PO_4$ decoupling inferred from the Cd* parameter

The Cd* parameter has been used as a tracer of seawater Cd enrichment or depletion relative to PO_4 and is calculated assuming a constant deep-water Cd/PO_4 ratio (e.g. Baars et al., 2014; Janssen et al., 2014):

$$Cd^* = Cd_{measured} - (Cd/PO_4)_{deep} \times PO_{4measured} \quad (2)$$

Regardless of the deep-water Cd/PO_4 ratio used in the calculation, positive and negative shifts of Cd* in general indicate enrichment and depletion of Cd compared to PO_4, respectively. For example, strong covariation of Fe or Mn concentrations in Southern Ocean surface waters with Cd*, and Cd isotopes as well, has been related to changes in the Cd:PO_4 uptake rate and the mechanisms of cellular uptake, which are controlled by the availability of micronutrient trace metals (Abouchami et al., 2011; Baars et al., 2014). Additionally, negative shifts of Cd* have helped identify ODZ waters as possible oceanic Cd sinks (Conway and John, 2015a; Conway and John, 2015b; Janssen et al., 2017; Janssen et al., 2014; Waeles et al., 2016).

As pointed out by Middag et al. (2018), however, using a constant deep-water Cd/PO_4 ratio for an entire ocean basin might not be suitable in areas where the oxygen deficit or remineralization is high. For example, although negative subsurface shifts in Cd* coincide with samples that display lower-than-expected Cd in a Cd-PO4 cross plot for the tropical Atlantic water column (GA11, this study; GA03, Conway and John, 2015a and Janssen et al., 2014) (Fig. S5), similarly negative shifts in Cd* are also observed at stations where no such $Cd\text{-}PO_4$ decoupling was previously observed from $Cd\text{-}PO_4$ cross plots, such as St. 6 along GA02 in the Southwest Atlantic (Xie et al., 2015) (Fig. S5). In this case, the occurrence of negative Cd* signatures is independent of the

presence or lack of decoupling between Cd and PO_4, as inferred from a Cd-PO_4 cross plot.

In summary, the significance of the Cd* tracer will depend strongly on the local water column biogeochemistry and the particulate compositions, their origins and concentrations, in agreement with the conclusion of Middag et al. (2018). Thus, it is essential that these additional parameters are taken into consideration for interpreting local versus global oceanic Cd-PO_4 correlations.

5. Conclusions

We report coupled Cd concentration and Cd isotopic compositions from six seawater profiles and six tow-fish surface water sites along the GEOTRACES GA11 section from the northeastern to southwestern tropical Atlantic. This new dataset is used to evaluate the significance of riverine and eolian Cd input to the open ocean Cd isotope budget.

Although the Amazon River is the world's largest river by discharge, our surface seawater samples taken at the margin of the Amazon plume show no discernable differences in either Cd concentration or isotopic compositions compared to surface waters from other oceanic regions, suggesting insignificant riverine Cd contributions to the open ocean. Any quantification of riverine inputs will, however, require a dedicated study covering the entire salinity gradient. We also show that atmospheric input of Cd to the eastern tropical North Atlantic via the African dust plume amounts to < 1% of the inferred upwelling Cd flux.

Local riverine and eolian sources do not seem to impact directly on the Cd biogeochemical cycle, even in the extreme cases of Amazon River discharge and the African dust outflow. Nevertheless, these local sources will strongly influence the productivity in areas limited by availability of other micronutrients, such as Fe and Zn, and will indeed be driven by these inputs. Thus, the uptake and cycling of Cd in these regions will inevitably be affected collaterally, in an indirect manner, by eolian and riverine sources. Furthermore, these sources of Cd must to some extent be important, since they are required to balance the sedimentary sinks in the long-term Cd cycle in the oceans.

The distributions of Cd and its isotopes in the tropical Atlantic are largely controlled by internal biogeochemical cycling and ocean circulation. In the intermediate and deep tropical North Atlantic, water mass mixing explains satisfactorily the GA11 [Cd] and δ^{114}Cd distribution. The significant deviation toward lower Cd at given PO_4 for samples at 100–200 m from the tropical stations indicates that the decoupling between Cd and PO_4 is a common feature of the tropical Atlantic. Preferential removal of isotopically light Cd in the form of CdS may explain the lower-than-expected [Cd] of ODZ waters. Alternatively, preferential re-mineralization of particulate organic phosphorus versus particulate Cd may account for the Cd-PO_4 decoupling over the entire tropical Atlantic. Future studies on particle compositions and Cd speciation in ODZ waters and the tropical oceans will help to distinguish between these contrasting hypotheses.

Supplementary data to this article can be found online at https://doi.org/10.1016/j.chemgeo.2018.10.018.

Acknowledgements

We thank the Captain and crew of the RV Meteor, and the scientific party on-board GEOTRACES cruise GA11 (M81/1). Claudia Ehlert is thanked for her help in seawater sampling, Heinz Feldmann for keeping the TIMS lab going as well as Reimund Jotter and Siegfried Herrmann for their support in the clean lab. Jan van Oijen is particularly thanked for acquiring the nutrient dataset on the GA11 samples at short notice. We are grateful for the constructive comments from three anonymous reviewers, guest editor Tim Conway, and editor-in-chief Michael E. Böttcher. R.C.X. was supported by a Max Planck Society fellowship. W. A. was funded by UnivEarths LABEX program at Sorbonne Paris Cité (ANR-10-LABEX-0023 and ANR-11-IDEX-0005-02).

References

Abouchami, W., Galer, S.J.G., de Baar, H.J.W., Alderkamp, A.C., Middag, R., Laan, P., Feldmann, H., Andreae, M.O., 2011. Modulation of the Southern Ocean cadmium isotope signature by ocean circulation and primary productivity. Earth Planet. Sci. Lett. 305 (1), 83–91.

Abouchami, W., Galer, S.J.G., Horner, T.J., Rehkämper, M., Wombacher, F., Xue, Z., Lambelet, M., Gault-Ringold, M., Stirling, C.H., Schönbächler, M., Shiel, A.E., Weis, D., Holdship, P.F., 2013. A common reference material for cadmium isotope studies–NIST SRM 3108. Geostand. Geoanal. Res. 37 (1), 5–17.

Abouchami, W., Galer, S.J.G., de Baar, H.J.W., Middag, R., Vance, D., Zhao, Y., Klunder, M., Mezger, K., Feldmann, H., Andreae, M.O., 2014. Biogeochemical cycling of cadmium isotopes in the Southern Ocean along the Zero Meridian. Geochim. Cosmochim. Acta 127 (0), 348–367.

Baars, O., Abouchami, W., Galer, S.J.G., Boye, M., Croot, P.L., 2014. Dissolved cadmium in the Southern Ocean: distribution, speciation, and relation to phosphate. Limnol. Oceanogr. 59 (2), 385–399.

Bianchi, D., Weber, T.S., Kiko, R., Deutsch, C., 2018. Global niche of marine anaerobic metabolisms expanded by particle microenvironments. Nat. Geosci. 11 (4), 263.

Boyle, E.A., Huested, S.S., Grant, B., 1982. The chemical mass balance of the amazon plume—II. Copper, nickel, and cadmium. Deep Sea Res. Part A 29 (11), 1355–1364.

Boyle, E.A., John, S., Abouchami, W., Adkins, J.F., Echegoyen-Sanz, Y., Ellwood, M., Flegal, A.R., Fornace, K., Gallon, C., Galer, S., 2012. GEOTRACES IC1 (BATS) contamination-prone trace element isotopes Cd, Fe, Pb, Zn, Cu, and Mo intercalibration. Limnol. Oceanogr. Methods 10 (9), 653–665.

Bridgestock, L., Rehkämper, M., van de Flierdt, T., Murphy, K., Khondoker, R., Baker, A.R., Chance, R., Strekopytov, S., Humphreys-Williams, E., Achterberg, E.P., 2017. The Cd isotope composition of atmospheric aerosols from the Tropical Atlantic Ocean. Geophys. Res. Lett. 44 (6), 2932–2940.

Bruland, K.W., 1980. Oceanographic distributions of cadmium, zinc, nickel, and copper in the North Pacific. Earth Planet. Sci. Lett. 47 (2), 176–198.

Chrastný, V., Čadková, E., Vaněk, A., Teper, L., Cabala, J., Komárek, M., 2015. Cadmium isotope fractionation within the soil profile complicates source identification in relation to Pb–Zn mining and smelting processes. Chem. Geol. 405, 1–9.

Cloquet, C., Carignan, J., Libourel, G., Sterckeman, T., Perdrix, E., 2006. Tracing source pollution in soils using cadmium and lead isotopes. Environ. Sci. Technol. 40 (8), 2525–2530.

Conway, T.M., John, S.G., 2015a. Biogeochemical cycling of cadmium isotopes along a high-resolution section through the North Atlantic Ocean. Geochim. Cosmochim. Acta 148, 269–283.

Conway, T.M., John, S.G., 2015b. The cycling of iron, zinc and cadmium in the North East Pacific Ocean – insights from stable isotopes. Geochim. Cosmochim. Acta 164, 262–283.

Cullen, J.T., Maldonado, M.T., 2013. Biogeochemistry of Cadmium and Its Release to the Environment, Cadmium: From Toxicity to Essentiality. Springer, pp. 31–62.

Duce, R.A., Liss, P.S., Merrill, J.T., Atlas, E.L., Buat-Menard, P., Hicks, B.B., Miller, J.M., Prospero, J.M., Arimoto, R., Church, T.M., Ellis, W., Galloway, J.N., Hansen, L., Jickells, J.D., Knap, A.H., Reinhardt, K.H., Schneider, B., Soudine, A., Tokos, J.J., Tsunogai, S., Wollast, W., Zhou, M., 1991. The atmospheric input of trace species to the world ocean. Glob. Biogeochem. Cycles 5 (3), 193–259.

Engel, A., Wagner, H., Le Moigne, F.A., Wilson, S.T., 2017. Particle export fluxes to the oxygen minimum zone of the eastern Tropical North Atlantic. Biogeosciences 14 (7), 1825.

Fischer, G., Karakaş, G., 2009. Sinking rates and ballast composition of particles in the Atlantic Ocean: implications for the organic carbon fluxes to the deep ocean. Biogeosciences 6 (1), 85–102.

Gaillardet, J., Viers, J., Dupré, B., 2014. 7.7 - Trace elements in river waters A2 - Holland, Heinrich D. In: Turekian, K.K. (Ed.), Treatise on Geochemistry, Second edition. Elsevier, Oxford, pp. 195–235.

Gao, B., Liu, Y., Sun, K., Liang, X., Peng, P.a., Sheng, G., Fu, J., 2008. Precise determination of cadmium and lead isotopic compositions in river sediments. Anal. Chim. Acta 612 (1), 114–120.

Gao, B., Zhou, H., Liang, X., Tu, X., 2013. Cd isotopes as a potential source tracer of metal pollution in river sediments. Environ. Pollut. 181, 340–343.

Garcia, H.E., Locarnini, R.A., Boyer, T.P., Antonov, J.I., Baranova, O.K., Zweng, M.M., Reagan, J.R., Johnso, D.R., 2014. World Ocean Atlas 2013. In: Levitus, S. (Ed.), Dissolved Oxygen, Apparent Oxygen Utilization, and Oxygen Saturation. NOAA Atlas NESDIS 75, vol. 3 27 pp.

Gault-Ringold, M., Adu, T., Stirling, C.H., Frew, R.D., Hunter, K.A., 2012. Anomalous biogeochemical behavior of cadmium in subantarctic surface waters: Mechanistic constraints from cadmium isotopes. Earth Planet. Sci. Lett. 341–344, 94–103.

Grasshoff, K., Kremling, K., Ehrhardt, M., 2009. Methods of Seawater Analysis. John Wiley & Sons.

Guinoiseau, D., Galer, S.J.G., Abouchami, W., 2018. Effect of cadmium sulphide precipitation on the partitioning of Cd isotopes: implications for the oceanic Cd cycle. Earth Planet. Sci. Lett. 498, 300–308.

Janssen, D.J., Conway, T.M., John, S.G., Christian, J.R., Kramer, D.I., Pedersen, T.F., Cullen, J.T., 2014. Undocumented water column sink for cadmium in open ocean oxygen-deficient zones. Proc. Natl. Acad. Sci. 111 (19), 6888–6893.

Janssen, D.J., Abouchami, W., Galer, S.J.G., Cullen, J.T., 2017. Fine-scale spatial and interannual cadmium isotope variability in the subarctic northeast Pacific. Earth Planet. Sci. Lett. 472, 241–252.

Jenkins, W.J., Smethie Jr., W.M., Boyle, E.A., Cutter, G.A., 2015. Water mass analysis for the U.S. GEOTRACES (GA03) North Atlantic sections. Deep-Sea Res. II Top. Stud. Oceanogr. 116 (0), 6–20.

John, S.G., Helgoe, J., Townsend, E., 2017. Biogeochemical cycling of Zn and Cd and their stable isotopes in the Eastern Tropical South Pacific. Mar. Chem. 201, 66–76.
Karstensen, J., Stramma, L., Visbeck, M., 2008. Oxygen minimum zones in the eastern Tropical Atlantic and Pacific oceans. Prog. Oceanogr. 77 (4), 331–350.
Kuss, J., Kremling, K., 1999. Spatial variability of particle associated trace elements in near-surface waters of the North Atlantic (30°N/60°W to 60°N/2°W), derived by large volume sampling. Mar. Chem. 68 (1), 71–86.
Lambelet, M., Rehkämper, M., van de Flierdt, T., Xue, Z., Kreissig, K., Coles, B., Porcelli, D., Andersson, P., 2013. Isotopic analysis of Cd in the mixing zone of Siberian rivers with the Arctic Ocean - new constraints on marine Cd cycling and the isotope composition of riverine Cd. Earth Planet. Sci. Lett. 361, 64–73.
Li, Y.-H., 1982. A brief discussion on the mean oceanic residence time of elements. Geochim. Cosmochim. Acta 46 (12), 2671–2675.
Mahowald, N.M., Engelstaedter, S., Luo, C., Sealy, A., Artaxo, P., Benitez-Nelson, C., Bonnet, S., Chen, Y., Chuang, P.Y., Cohen, D.D., 2009. Atmospheric iron deposition: global distribution, variability, and human perturbations. Annu. Rev. Mar. Sci. 1, 245–278.
Martin, J.-M., Whitfield, M., 1983. The significance of the river input of chemical elements to the ocean. In: Wong, C.S., Boyle, E., Bruland, K.W., Burton, J.D., Goldberg, E.D. (Eds.), Trace Metals in Sea Water. NATO Conference Series (IV Marine Sciences), vol. 9 Springer, Boston, MA.
Middag, R., De Baar, H., Laan, P., Bakker, K., 2009. Dissolved aluminium and the silicon cycle in the Arctic Ocean. Mar. Chem. 115 (3), 176–195.
Middag, R., van Heuven, S.M.A.C., Bruland, K.W., de Baar, H.J.W., 2018. The relationship between cadmium and phosphate in the Atlantic Ocean unravelled. Earth Planet. Sci. Lett. 492, 79–88.
Mills, M.M., Ridame, C., Davey, M., La Roche, J., Geider, R.J., 2004. Iron and phosphorus co-limit nitrogen fixation in the eastern Tropical North Atlantic. Nature 429 (6989), 292–294.
Ohnemus, D.C., Rauschenberg, S., Cutter, G.A., Fitzsimmons, J.N., Sherrell, R.M., Twining, B.S., 2017. Elevated trace metal content of prokaryotic communities associated with marine oxygen deficient zones. Limnol. Oceanogr. 62 (1), 3–25.
Ripperger, S., Rehkämper, M., Porcelli, D., Halliday, A., 2007. Cadmium isotope fractionation in seawater—a signature of biological activity. Earth Planet. Sci. Lett. 261 (3), 670–684.
Roshan, S., Wu, J., 2015. Cadmium regeneration within the North Atlantic. Glob. Biogeochem. Cycles 29 (12), 2082–2094.
Schlitzer, R., 2014. Ocean data view. http://odv.awi.de.
Schlitzer, R., Anderson, R.F., Dodas, E.M., Lohan, M., Geibert, W., Tagliabue, A., Bowie, A., Jeandel, C., Maldonado, M.T., Landing, W.M., Cockwell, D., Abadie, C., Abouchami, W., Achterberg, E.P., Agather, A., Aguliar-Islas, A., van Aken, H.M., Andersen, M., Archer, C., Auro, M., de Baar, H.J., Baars, O., Baker, A.R., Bakker, K., Basak, C., Baskaran, M., Bates, N.R., Bauch, D., van Beek, P., Behrens, M.K., Black, E., Bluhm, K., Bopp, L., Bouman, H., Bowman, K., Bown, J., Boyd, P., Boye, M., Boyle, E.A., Branellec, P., Bridgestock, L., Brissebrat, G., Browning, T., Bruland, K.W., Brumsack, H.-J., Brzezinski, M., Buck, C.S., Buck, K.N., Buesseler, K., Bull, A., Butler, E., Cai, P., Mor, P.C., Cardinal, D., Carlson, C., Carrasco, G., Casacuberta, N., Casciotti, K.L., Castrillejo, M., Chamizo, E., Chance, R., Charette, M.A., Chaves, J.E., Cheng, H., Chever, F., Christl, M., Church, T.M., Closset, I., Colman, A., Conway, T.M., Cossa, D., Croot, P., Cullen, J.T., Cutter, G.A., Daniels, C., Dehairs, F., Deng, F., Dieu, H.T., Duggan, B., Dulaquais, G., Dumousseaud, C., Echegoyen-Sanz, Y., Edwards, R.L., Ellwood, M., Fahrbach, E., Fitzsimmons, J.N., Russell Flegal, A., Fleisher, M.Q., van de Flierdt, T., Frank, M., Friedrich, J., Fripiat, F., Fröllje, H., Galer, S.J.G., Gamo, T., Ganeshram, R.S., Garcia-Orellana, J., Garcia-Solsona, E., Gault-Ringold, M., George, E., Gerringa, L.J.A., Gilbert, M., Godoy, J.M., Goldstein, S.L., Gonzalez, S.R., Grissom, K., Hammerschmidt, C., Hartman, A., Hassler, C.S., Hathorne, E.C., Hatta, M., Hawco, N., Hayes, C.T., Heimbürger, L.-E., Helgoe, J., Heller, M., Henderson, G.M., Henderson, P.B., van Heuven, S., Ho, P., Horner, T.J., Hsieh, Y.-T., Huang, K.-F., Humphreys, M.P., Isshiki, K., Jacquot, J.E., Janssen, D.J., Jenkins, W.J., John, S., Jones, E.M., Jones, J.L., Kadko, D.C., Kayser, R., Kenna, T.C., Khondoker, R., Kim, T., Kipp, L., Klar, J.K., Klunder, M., Kretschmer, S., Kumamoto, Y., Laan, P., Labatut, M., Lacan, F., Lam, P.J., Lambelet, M., Lamborg, C.H., Le Moigne, F.A.C., Le Roy, E., Lechtenfeld, O.J., Lee, J.-M., Lherminier, P., Little, S., López-Lora, M., Lu, Y., Masque, P., Mawji, E., McClain, C.R., Measures, C., Mehic, S., Barraqueta, J.-L.M., van der Merwe, P., Middag, R., Mieruch, S., Milne, A., Minami, T., Moffett, J.W., Moncoiffe, G., Moore, W.S., Morris, P.J., Morton, P.L., Nakaguchi, Y., Nakayama, N., Niedermiller, J., Nishioka, J., Nishiuchi, A., Noble, A., Obata, H., Ober, S., Ohnemus, D.C., van Ooijen, J., O'Sullivan, J., Owens, S., Pahnke, K., Paul, M., Pavia, F., Pena, L.D., Peters, B., Planchon, F., Planquette, H., Pradoux, C., Puigcorbé, V., Quay, P., Queroue, F., Radic, A., Rauschenberg, S., Rehkämper, M., Rember, R., Remenyi, T., Resing, J.A., Rickli, J., Rigaud, S., Rijkenberg, M.J.A., Rintoul, S., Robinson, L.F., Roca-Martí, M., Rodellas, V., Roeske, T., Rolison, J.M., Rosenberg, M., Roshan, S., Rutgers Van Der Loeff, M.M., Ryabenko, E., Saito, M.A., Salt, L.A., Sanial, V., Sarthou, G., Schallenberg, C., Schauer, U., Scher, H., Schlosser, C., Schnetger, B., Scott, P., Sedwick, P.N., Semiletov, I., Shelley, R., Sherrell, R.M., Shiller, A.M., Sigman, D.M., Singh, S.K., Slagter, H.A., Slater, E., Smethie, W.M., Snaith, H., Sohrin, Y., Sohst, B., Sonke, J.E., Speich, S., Steinfeldt, R., Stewart, G., Stichel, T., Stirling, C.H., Stutsman, J., Swarr, G.J., Swift, J.H., Thomas, A., Thorne, K., Till, C.P., Till, R., Townsend, A.T., Townsend, E., Tuerena, R., Twining, B.S., Vance, D., Velazquez, S., Venchiarutti, C., Villa-Alfageme, M., Vivancos, S.M., Voelker, A.H.L., Wake, B., Warner, M.J., Watson, R., van Weerlee, E., Alexandra Weigand, M., Weinstein, Y., Weiss, D., Wisotzki, A., Woodward, E.M.S., Wu, J., Wu, Y., Wuttig, K., Wyatt, N., Xiang, Y., Xie, R.C., Xue, Z., Yoshikawa, H., Zhang, J., Zhang, P., Zhao, Y., Zheng, L., Zheng, X.-Y., Zieringer, M., Zimmer, L.A., Ziveri, P., Zunino, P., Zurbrick, C., 2018. The GEOTRACES Intermediate Data Product 2017. Chem. Geol. 493, 210–223.
Schmitt, A.-D., Galer, S.J.G., Abouchami, W., 2009. Mass-dependent cadmium isotopic variations in nature with emphasis on the marine environment. Earth Planet. Sci. Lett. 277 (1), 262–272.
Seyler, P.T., Boaventura, G.R., 2003. Distribution and partition of trace metals in the Amazon basin. Hydrol. Process. 17, 1345–1361.
Sieber, M., Conway, T., de Souza, G., Obata, H., Takano, S., Sohrin, Y., Vance, D., 2018. Physical and biogeochemical controls on the distribution of dissolved cadmium and its isotopes in the Southwest Pacific Ocean. Chem. Geol. https://doi.org/10.1016/j.chemgeo.2018.07.021.
Taylor, S.R., McLennan, S.M., 1985. The Continental Crust: Its Composition and Evolution. Blackwell Scientific Publications, United States, pp. 1–328.
Tovar-Sanchez, A., Sañudo-Wilhelmy, S.A., 2011. Influence of the Amazon River on dissolved and intra-cellular metal concentrations in Trichodesmium colonies along the western boundary of the sub-Tropical North Atlantic Ocean. Biogeosciences 8 (1), 217–225.
Twining, B.S., Rauschenberg, S., Morton, P.L., Vogt, S., 2015. Metal contents of phytoplankton and labile particulate material in the North Atlantic Ocean. Prog. Oceanogr. 137 (Part A), 261–283.
Viers, J., Dupré, B., Gaillardet, J., 2009. Chemical composition of suspended sediments in World Rivers: new insights from a new database. Sci. Total Environ. 407 (2), 853–868.
Waeles, M., Maguer, J.-F., Baurand, F., Riso, R.D., 2013. Off Congo waters (Angola Basin, Atlantic Ocean): a hot spot for cadmium-phosphate fractionation. Limnol. Oceanogr. 58 (4), 1481–1490.
Waeles, M., Planquette, H., Afandi, I., Delebecque, N., Bouthir, F., Donval, A., Shelley, R.U., Auger, P.A., Riso, R.D., Tito De Morais, L., 2016. Cadmium in the waters off South Morocco: nature of particles hosting Cd and insights into the mechanisms fractionating Cd from phosphate. J. Geophys. Res. Oceans 121 (5), 3106–3120.
Wu, J., Roshan, S., 2015. Cadmium in the North Atlantic: implication for global cadmium–phosphorus relationship. Deep-Sea Res. II Top. Stud. Oceanogr. 116 (0), 226–239.
Wunsch, C., 1984. An estimate of the upwelling rate in the equatorial Atlantic based on the distribution of bomb radiocarbon and quasi-geostrophic dynamics. J. Geophys. Res. Oceans 89 (C5), 7971–7978.
Xie, R.C., Galer, S.J.G., Abouchami, W., Rijkenberg, M.J.A., De Jong, J., de Baar, H.J.W., Andreae, M.O., 2015. The cadmium–phosphate relationship in the western South Atlantic - the importance of mode and intermediate waters on the global systematics. Mar. Chem. 177 (Part 1), 110–123.
Xie, R.C., Galer, S.J.G., Abouchami, W., Rijkenberg, M.J., de Baar, H.J., De Jong, J., Andreae, M.O., 2017. Non-Rayleigh control of upper-ocean Cd isotope fractionation in the western South Atlantic. Earth Planet. Sci. Lett. 471, 94–103.
Xie, R.C., Rehkämper, M., Grasse, P., van de Flierd, T., Frank, M., Xue, Z., 2018. Subsurface Cd depletion in the eastern tropical South Pacific oxygen minimum zone. Earth Planet. Sci. Lett (in review).
Xue, Z., Rehkämper, M., Schönbächler, M., Statham, P., Coles, B., 2012. A new methodology for precise cadmium isotope analyses of seawater. Anal. Bioanal. Chem. 402 (2), 883–893.
Xue, Z., Rehkämper, M., Horner, T.J., Abouchami, W., Middag, R., van de Flierd, T., de Baar, H.J.W., 2013. Cadmium isotope variations in the Southern Ocean. Earth Planet. Sci. Lett. 382, 161–172.
Yang, J., Li, Y., Liu, S., Tian, H., Chen, C., Liu, J., Shi, Y., 2015. Theoretical calculations of Cd isotope fractionation in hydrothermal fluids. Chem. Geol. 391, 74–82.
Yang, W.J., Ding, K.B., Zhang, P., Qiu, H., Cloquet, C., Wen, H.J., Morel, J.L., Qiu, R.L., Tang, Y.T., 2019. Cadmium stable isotope variation in a mountain area impacted by acid mine drainage. Sci. Total Environ. 646, 696–703.
Zhang, Y., Wen, H., Zhu, C., Fan, H., Luo, C., Liu, J., Cloquet, C., 2016. Cd isotope fractionation during simulated and natural weathering. Environ. Pollut. 216, 9–17.